

# Some observations on interactions between unstressed AISI 304L steel and zinc or zinc oxide

R. M. CRISPIN, M. G. NICHOLAS

*Materials Development Division, AERE, Harwell, Oxfordshire*

A laboratory study has been made of the interactions of unstressed AISI 304L stainless steel with zinc and zinc oxide in air, carbon monoxide or argon-hydrogen. Erosion or penetration ranging from 0.003 to 1.7 mm was produced by molten zinc in 1 h at 500 to 850° C in air and argon-hydrogen. The penetration at 700 to 850° C formed mechanically detrimental structures such as cracked intermetallic layers, distorted and fissured interdiffusion zones and liquid channels. No penetration occurred in carbon monoxide atmospheres because of the deposition of a carbon barrier layer onto the steel surfaces. Similarly, thick oxide films could delay penetration. Zinc vapour and zinc oxide produced pitting of the steel surfaces, the attack by zinc oxide being the more severe.

## 1. Introduction

This paper describes a study of some aspects of the interaction of AISI 304L stainless steel with zinc and zinc oxide. The potential importance of interactions between austenitic stainless steels and zinc or zinc compounds has been revealed by, for example, the investigation of a hydrocarbon plant fire described by Cantwell and Bryant [1] and particularly by the evidence submitted to the Court of Inquiry into the Flixborough Disaster showing that AISI 316L stainless steel was embrittled by molten zinc at high temperatures [2]. That evidence led to a widespread concern in the UK [3, 4] about the harmful effects of zinc, the issue of a circular by the UK Health and Safety Executive [5] and the initiation of research programmes by several major UK and European organisations to obtain additional information of relevance to their plant materials and conditions.

Elliott [6] and Sadigh [7] summarized the conditions under which zinc-stainless steel interactions have been reported to occur and Cottrell and Swann [8] have identified two processes by which embrittlement can be produced; a fast process that merely requires crack faces to be wetted by zinc, and a slow process that requires zinc to penetrate into the body of the stainless steel. The first has been observed to occur at

750 to 1000° C [1, 8-11] and the second at 570° C and above [9-14]. However, there is some evidence suggesting that the penetration process can be inhibited or delayed by oxide layers on AISI 316L stainless steel surfaces or by carburizing atmospheres [8, 12].

This possibility has led to the study described in this paper which attempted to obtain additional information about the kinetics and effects of environment on zinc-austenitic steel interactions. Experiments were conducted to define the rates at which molten zinc or zinc vapour penetrated unstressed AISI 304L stainless steel at 500 to 850° C in air, the effects of changing from air to carbon monoxide or argon-hydrogen atmospheres, and of replacing zinc by zinc oxide.

## 2. Experimental materials and techniques

The materials used in this work were of commercial quality. The composition of the AISI 304L steel is given in Table I, while the purities of the zinc and zinc oxide were 99.94 and 99.7%, respectively. The carbon monoxide environment used in a few experiments was 99.5% pure, the composition of the argon-hydrogen mixture used in two series of experiments is given in Table II.

Steel samples were prepared by cutting 8 mm side squares from a cold rolled sheet, abrading

TABLE I Nominal composition of the AISI 304L stainless steel

Element	Composition (wt %)
Chromium	19.0
Nickel	10.4
Manganese	1.3
Silicon	0.7
Carbon	0.03
Iron	Balance

their surfaces with 600 grade SiC, ultrasonically degreasing in methylated spirits and heating in evacuated silica capsules to 1000° C for 3 h. Zinc droplets were ejected onto the surfaces of such samples at predetermined temperatures by squeezing the rubber bulk of the device sketched in Fig. 1.\* The temperatures within the device were related to furnace settings by calibration runs using thermocouples placed within the empty dispenser tube and alumina crucible, and between the crucible and the container vessel. The temperatures were monitored during the actual experiments by the thermocouple between the crucible and the container vessel. A steel sample was placed in the alumina crucible and 1.5 gm of zinc was put in the dispenser tube before it was placed in a vertical muffle furnace heated to 500 to 850° C. If the experiments were to be conducted using carbon monoxide or argon-hydrogen atmospheres, the zinc granules were melted to seal the end of the dispenser which was then evacuated, purged and filled with the appropriate gas before being inserted in the muffle furnace. Zinc was ejected onto the steel, usually 10 min after the steel and molten zinc had been stabilized at the same temperature and allowed to remain in contact for some time, usually 1 h, before the whole device

TABLE II Composition of the argon-hydrogen gas mixture

Gas	Composition (%)
Hydrogen	4.80
Nitrogen	0.06
Oxygen	0.008
Carbon dioxide	0.003
Argon	95.10

\*The pressures needed to eject zinc at 500° C through 1.5 mm diameter holes were measured with a manometer attachment during preliminary experiments and were found to be less than 1 Ncm<sup>-2</sup> for silica tubes and 5 to 20 Ncm<sup>-2</sup> for less wetted alumina tubes. When zinc was ejected from alumina in air, the pressure release was caused by a distinct bang and also was accompanied by a light green flash and white smoke which was considered potentially hazardous. Silica was selected as the dispenser tube material when analysis of ejected droplets failed to reveal any evidence of silicon contamination.

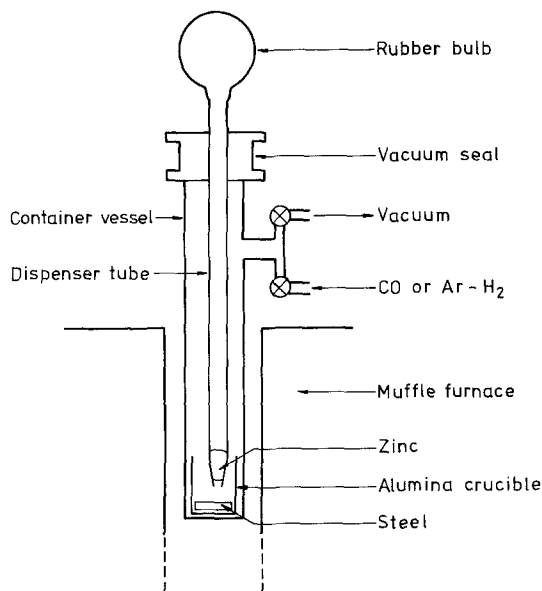


Figure 1 Device for ejecting molten zinc onto steel samples.

was removed from the muffle furnace and the sample allowed to cool.

A large electrically heated air furnace was used to produce samples defining the interaction of zinc vapour and zinc oxide with stainless steel. The vapour experiments were conducted in still air using the simple crucible arrangement sketched in Fig. 2. In the other experiments, steel samples at the bottom of alumina crucibles were covered with zinc powder to a depth of 5 to 10 mm before

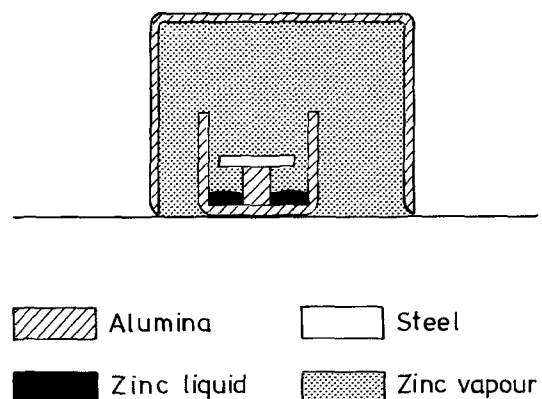


Figure 2 Arrangement used in zinc vapour studies.

being sealed in silica capsules filled with  $\frac{1}{4}$  atmosphere of argon–hydrogen.

The samples produced by these various methods were sectioned, polished and examined using optical microscopy before and after etching with nital or an HF–HNO<sub>3</sub>–H<sub>2</sub>O solution. The dimensions of the various features revealed before and after etching and those of the unattacked steel cores of the samples were measured from photomicrographs or using a digitized microscope stage with a resolution of  $\pm 0.001$  mm. A few of the polished cross-sections were assessed further using a Leitz microhardness tester and an electron probe microanalyser.

### 3. Results

#### 3.1. Zinc in air

Two series of experiments were conducted in which zinc droplets were ejected onto steel samples heated in air. In the principal series, the dispensing device was kept in the muffle furnace for 1 h after the zinc had been ejected and examination of the samples produced in this manner revealed three types of interaction behaviour.

(a) At 500°C, zinc flowed completely over the steel surfaces to form a layer about 0.1 mm thick but optical microscopy and electron probe microanalyser surveys did not reveal any indication of penetration into the steel, Fig. 3. Thickness measurements of the steel using a digitized microscope stage suggested that 0.003 mm erosion had occurred and electron probe microanalyser examinations showed that substrate components had dissolved in the zinc. The composition of the layer corresponded to Zn 17 at% Fe 6 at% Cr 1.6 at% Ni, suggesting that an intermetallic analogous to  $\Gamma$  FeZn<sub>3</sub> and  $\gamma'$  NiZn<sub>3</sub> had been formed [15].

(b) Samples produced at 700, 725 and 750°C were partially wetted, the zinc remaining as a globule attached to about a quarter of the sample surface. The micrographs in Fig. 4 show the penetration to have produced an angular layer adjacent to the droplet and a very distorted region adjacent to the steel. Both the layer and the distorted region contained cracks and fissures. Electron probe microanalyser surveys, such as that illustrated in Fig. 5, showed the layer to be a zinc rich intermetallic with a composition of Zn 18 at% Fe 5.6 at% Cr 1.4 at% Ni and the distorted region to be an interdiffusion zone. Further etching in an HF–HNO<sub>3</sub>–H<sub>2</sub>O mixture did not cause any change in the interdiffusion zone boundaries but

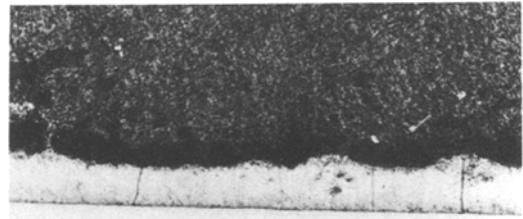


Figure 3 Cross-section of molten zinc–steel sample produced and held in air for 1 h at 500°C,  $\times 57.6$ . Etched in nital.

suggested that some features were related to the original grain structure of the steel. The material in the zone was harder than the steel, about 3000 MNm<sup>-2</sup> as compared to 1500 MNm<sup>-2</sup>, but its smaller density caused the zinc droplet to be raised above the steel surface. Increasing the experimental temperature enhanced the erosion and penetration as shown by the data in Table III.

(c) At temperatures of 800°C and above, the ejected zinc formed a globule occupying about half the sample surface and penetrated the substrate to form a channel and island structure. The islands had a hardness of about 2500 MNm<sup>-2</sup> and their rounded forms showed the channel material to have been liquid at the experimental temperatures. Electron probe microanalyser surveys showed the islands to contain iron, chromium and nickel in the approximate proportions of 74:24:2. The channels were mainly zinc, but also contained nickel, iron, manganese and chromium in the approximate proportions 62:24:7:7. The transition from this structure to unpenetrated steel was achieved in samples produced at 850°C by a gradual merging into a grain boundary penetration zone initially displaying zinc rich inclusions at grain corners, Fig. 6. The transition in samples produced at 800°C was through a distorted interdiffusion zone similar to that produced at 700 to 750°C, Fig. 7.

The depths,  $p$  (in mm), to which zinc penetrated during 1 h of contact varied monotonically with temperature,  $T$  (in K), as shown in Fig. 8, and can be represented by the equation

$$\log_{10} p = \frac{-6.63 \times 10^3}{T} + 6.08. \quad (1)$$

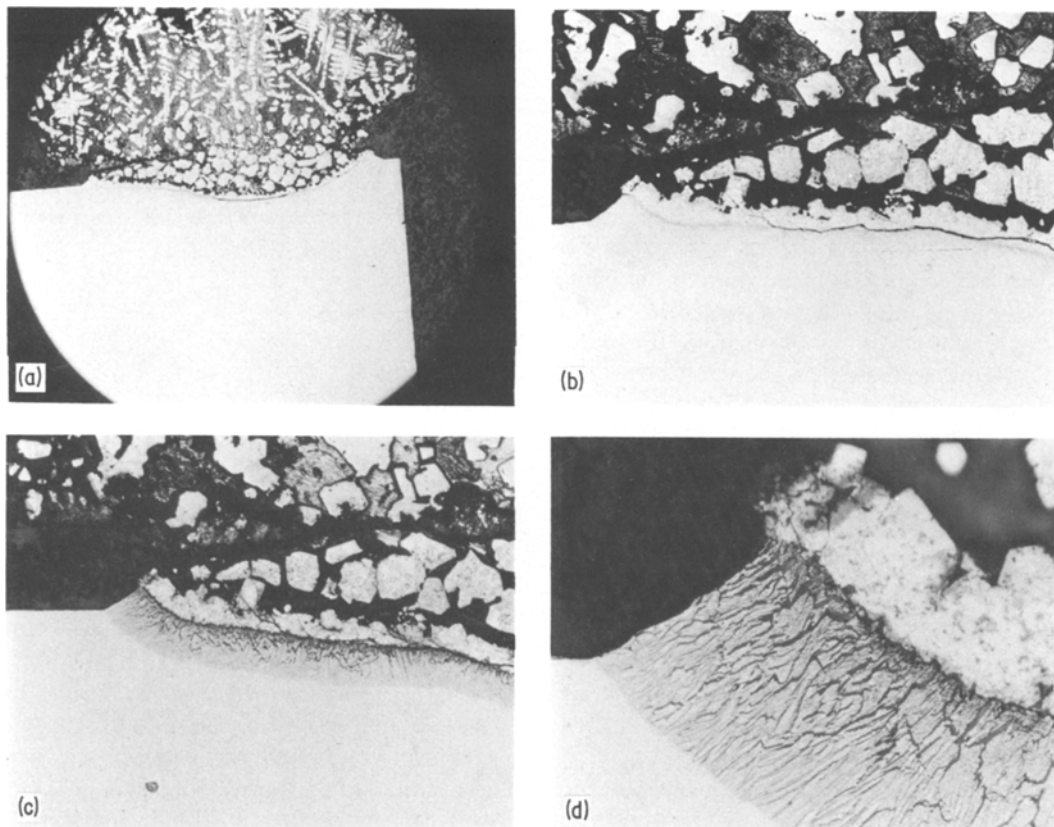


Figure 4 Cross-section of molten zinc-steel sample produced and held in air for 1 h at 750°C, (a) unetched,  $\times 7.2$  (b) unetched,  $\times 57.6$  (c) etched in nital,  $\times 57.6$  (d) etched in nital,  $\times 288$ .

The slope of the line drawn in Fig. 8 would correspond to an activation energy of about  $255 \text{ kJ g}^{-1} \text{ mol}^{-1}$  if the penetration process was a simple parabolic function of time. Examination of samples in which zinc was in contact with the steel for less than 1 h showed that the penetration did indeed vary with time but not in a simple manner. The parabolic function had to be modified to include an incubation period of 1.5 and 15 min at 700 and 850°C, Fig. 9. These delays were thought to be due to the inhibiting effects of oxide films, which microbalance weight gain measurements suggested were about 6, 35 and 90 nm thick after the normal 10 min holding times in air at 500, 700 and 850°C. If account is taken of these incubation times, the apparent activation energy for the penetration process is decreased to  $235 \text{ kJ mol}^{-1}$ .

### 3.2. Zinc vapour in air

Steel samples were exposed to zinc vapour in air at temperatures of 700 to 850°C for times of up to 1 h. There was no discernible erosion or build

up of zinc on the sample surfaces, but a few isolated pits formed which occupied perhaps 1% of the sample surfaces. The pit structures were complex, Fig. 10, and the readily etched regions within the steel close to the pit bottom were zinc rich but their smallness and infrequency made quantitative electron probe microanalysis difficult. Measurements made on cross-sectioned samples showed that the maximum extent of pitting penetration tended to increase with exposure time, Table IV.

### 3.3. Zinc in carbon monoxide and argon-hydrogen

The use of carbon monoxide atmospheres produced carbon deposition on the steel surfaces, estimated to be 150 to 200 nm after 10 min at 500 to 600°C, that prevented any zinc penetration, even after an hour's contact at 850°C. The only interaction produced was carburization to depths varying between 10 and 100  $\mu\text{m}$ .

No deposits were observed when argon-hydrogen atmospheres were used. The ejected zinc wetted the steel completely at all the experi-

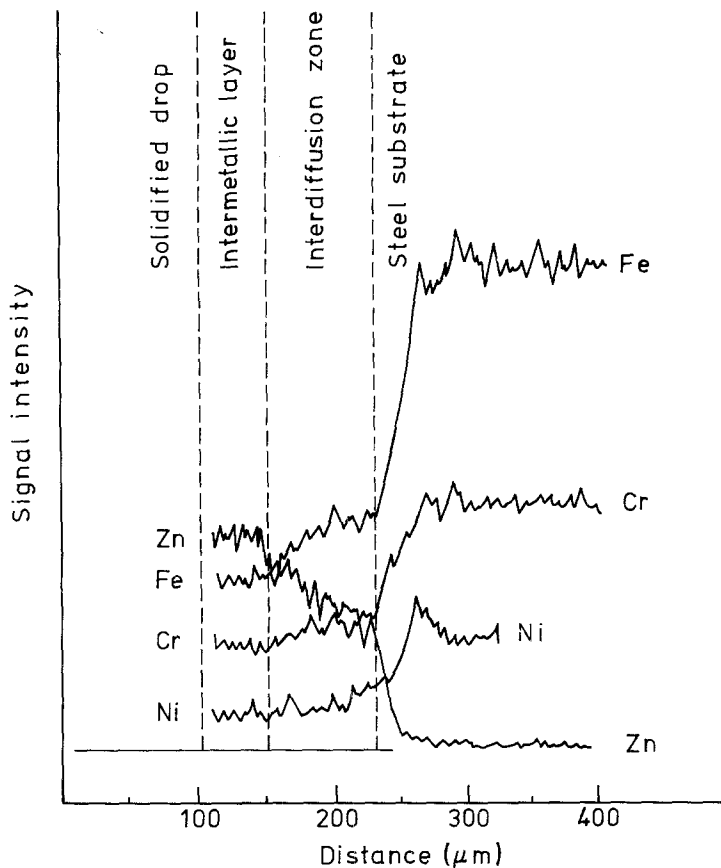


Figure 5 X-ray intensities observed during an electron probe microanalyser survey of a zinc-steel sample produced at 700° C.

mental temperatures and remained clean. Optical examination of cross-sectioned samples revealed structures similar to those observed previously for samples produced in air, as shown by the photomicrographs presented in Fig. 11. The only notable difference is that the channel and island structure was produced at 750° C and above in

argon-hydrogen rather than at 800° C and above as in air.

The extents of zinc penetration,  $p$  (in mm), revealed by these structural features, summarized in Table V, were slightly larger than those observed in air and were related to temperature,  $T$  (in K), by a similar simple function over the range 500 to

TABLE III Interaction data for steel heated in air for 10 min before being contacted by zinc for 60 min

Interaction temperature (°C)	Average values (mm)			
	Erosion	Intermetallic layer	Interdiffusion zone	Total penetration
500	0.003	< 0.001	< 0.001	0.003
	0.003	< 0.001	< 0.001	0.003
700	0.150	0.052	0.064	0.266
	0.175	0.052	0.052	0.279
725	0.200	0.050	0.052	0.302
750	0.350	0.042	0.104	0.496
	0.250	0.083	0.126	0.459
	Island and channel zone		Interdiffusion zone	Total penetration
800	1.13		0.020	1.150
	1.00		0.025	1.025
850	1.30		0.40	1.70
	1.30		0.30	1.60

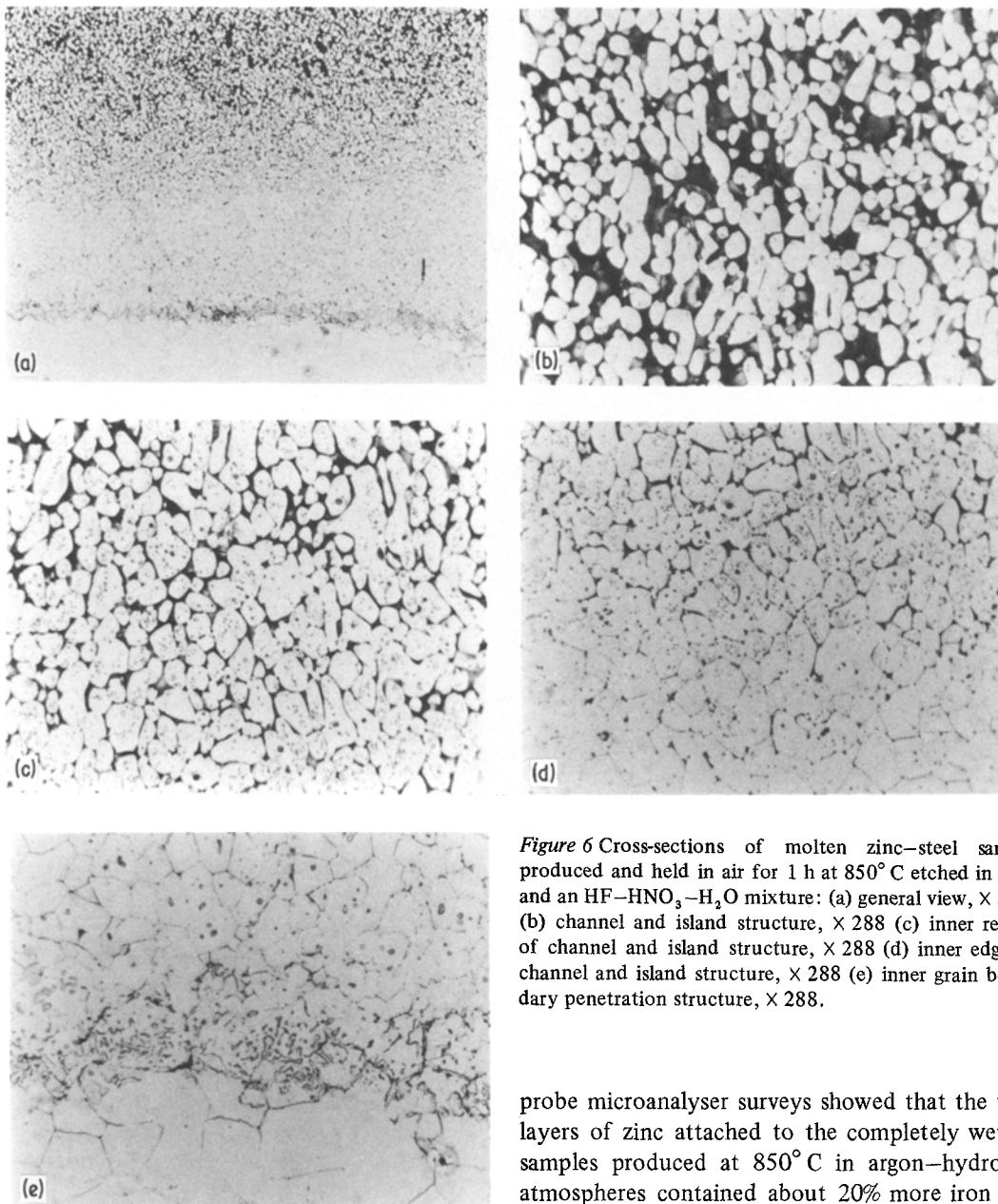


*Figure 6* Cross-sections of molten zinc–steel sample produced and held in air for 1 h at 850° C etched in nital and an HF–HNO<sub>3</sub>–H<sub>2</sub>O mixture: (a) general view, × 57.6 (b) channel and island structure, × 288 (c) inner region of channel and island structure, × 288 (d) inner edge of channel and island structure, × 288 (e) inner grain boundary penetration structure, × 288.

800° C, as shown by Fig. 12, that could be represented by the equation

$$\log_{10} p = \frac{-6 \times 10^3}{T} + 5.69. \quad (2)$$

This equation would suggest an activation energy of about 230 kJ g<sup>-1</sup> mol<sup>-1</sup> if the penetration process was a simple parabolic function of time.

The reason for the decreased penetration produced when the temperature was raised from 800 to 850° C was not established, but electron

probe microanalyser surveys showed that the thin layers of zinc attached to the completely wetted samples produced at 850° C in argon–hydrogen atmospheres contained about 20% more iron and chromium and almost ten times as much nickel as did the zinc globules on those produced in air.

### 3.4. Zinc oxide in argon–hydrogen

Interactions with zinc oxide in argon–hydrogen atmospheres were studied using steel samples heated at 700 to 850° C for up to 1 h. Several of the containment capsules exploded, but sufficient remained intact to permit behaviour to be defined. Contact with zinc oxide eroded the steel samples by 0.030 ± 0.022 mm as shown by the data assembled in Table VI. This erosion was accompanied by roughening of the surfaces from

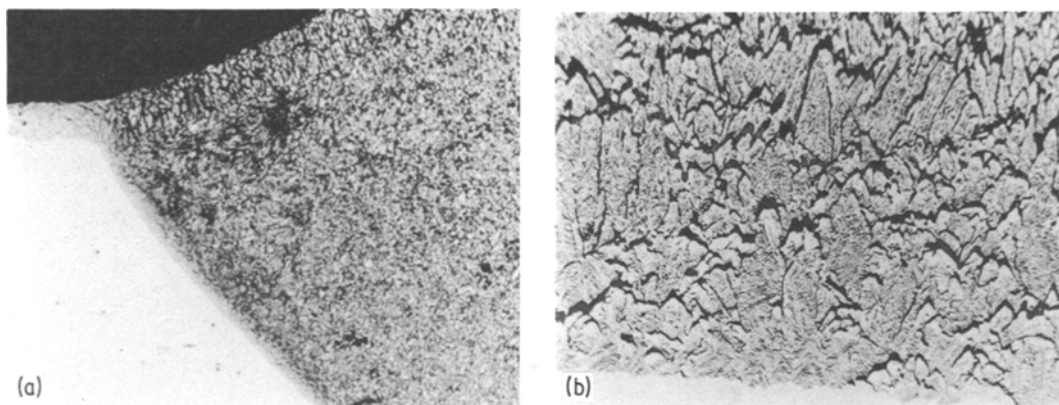


Figure 7 Cross-section of molten zinc-steel sample produced and held in air for 1 h at 800°C: (a) nitral etched,  $\times 57.6$  (b) nitral etched,  $\times 288$ .

an  $R_a$  value of 0.04 to 2 to 3  $\mu\text{m}$ . In places a thin surface phase was present that could be etched by nitral and, infrequently, a subsurface structure was observed similar to that produced by the zinc vapour interactions, Fig. 13. Electron probe microanalyser studies showed zinc to be associated with these features but their size did not permit quantitative analysis.

#### 4. Discussion

Some of the results presented in the previous section define relatively simple interaction phenomena that are consistent with other workers' obser-

ations. Thus three regimes of liquid zinc-steel interactions were revealed.

(a) Slow erosion without any penetration of the substrate at low temperatures, 500°C in this work and 419 to 570°C in that of Andreani *et al.* [9, 10]. Electron probe microanalysis data suggest that substrate components were taken into the zinc to produce a composition corresponding to  $(\text{FeCrNi})\text{Zn}_3$ , while Cordwell [13] reported that  $\text{NiZn}_3$  was formed at the surface of AISI 316 steel exposed to zinc vapour at 550°C.

(b) Erosion and uniform penetration of the substrate at moderate temperatures with the formation of a complex intermetallic layer, approximating to  $(\text{FeCrNi})\text{Zn}_3$ , at 700 to 750°C in air and at 700°C in argon-hydrogen at the surface

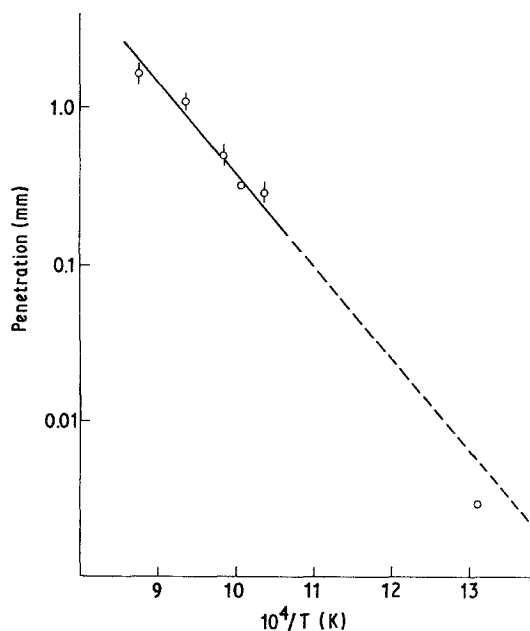


Figure 8 Plot of the penetration data as a function of temperature for steel samples in contact with zinc for 1 h in air.

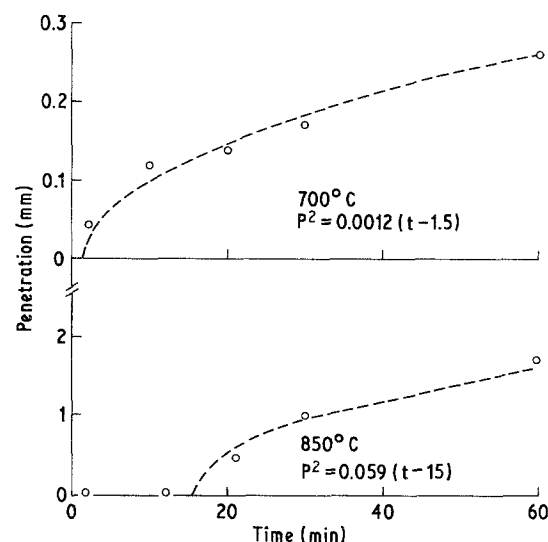


Figure 9 Penetration kinetics for the interaction of steel with molten zinc in air.

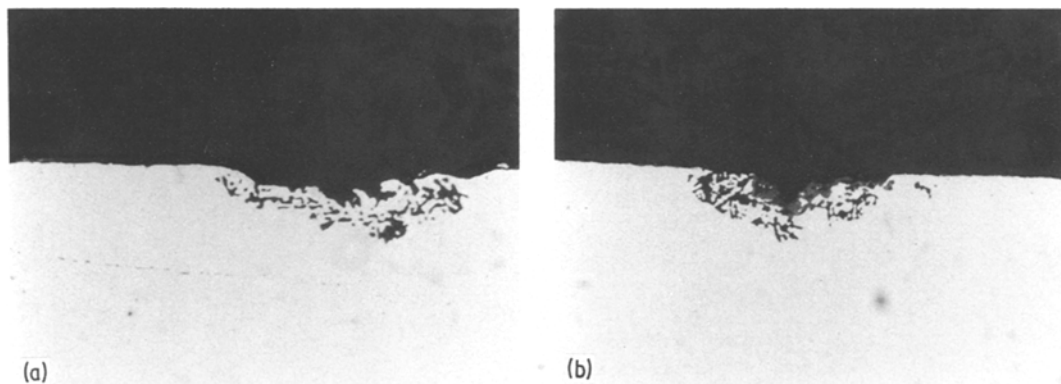


Figure 10 Pitting structures produced by exposing steel to zinc vapour (a) for 30 min at 700°C and (b) 20 min at 800°C. Etched in nital,  $\times 288$ .

of the steel and a distorted interdiffusion zone further in. Similarly, Andreani *et al.* [9, 10] observed significant penetration by zinc at 570 to 750°C, but not the formation of an intermetallic compound, and rearrangement to form nickel depleted grains surrounded by  $\beta$ -NiZn.

(c) Erosion and penetration of the substrate preferentially along grain boundaries with selective leaching of nickel at high temperatures, 800 to 850°C in air and 750 to 850°C in argon–hydrogen in this work and above 750°C in that of Andreani *et al.* [9, 10].

Observations made in this work on samples exposed for short times at high temperatures suggest that the moderate and high temperature phenomena are probably in fact merely different stages of the same zinc penetration process. The activation energy of this process derived from the rate data plotted in Fig. 9 is apparently 235 kJ

$\text{g}^{-1} \text{mol}^{-1}$ , in fair agreement with the 210 kJ  $\text{g}^{-1} \text{mol}^{-1}$  obtained by Andreani *et al.* [9] for the interdiffusion of nickel and zinc in an 18–10 austenitic stainless steel. Whatever penetration mechanism is involved, the resultant structural effects are of clear technical importance. Not only is steel consumed by the molten zinc, but the intermetallic layers produced at 700 to 750°C, and the distorted interdiffusion zones produced at 700 to 800°C, contained fissures and microcracks that could propagate to cause premature failure. The distortion and fissuring within the interdiffusion zone has not been studied in detail but could be due to the atomic radius mismatch of the penetrating zinc (0.137 nm zinc, 0.126 nm iron, 0.128 nm chromium, 0.125 nm nickel) or localized nickel depletion to cause an austenite–ferrite phase change and expansion as suggested by Andreani *et al.* [9]. The lack of

TABLE IV Interaction data for steel samples exposed to zinc vapour in air

Temperature (°C)	Exposure time (min)	Maximum penetration (mm)
700	10	0.023
	20	NP*
	30	0.027
	60	0.034
750	10	0.031
	20	0.021
	30	0.021
	60	0.021
800	10	0.017
	20	0.035
	30	0.031
	60	0.039
850	10	0.025
	20	NP*
	30	0.031
	60	0.038

\*NP – No pits observed in cross-sections.

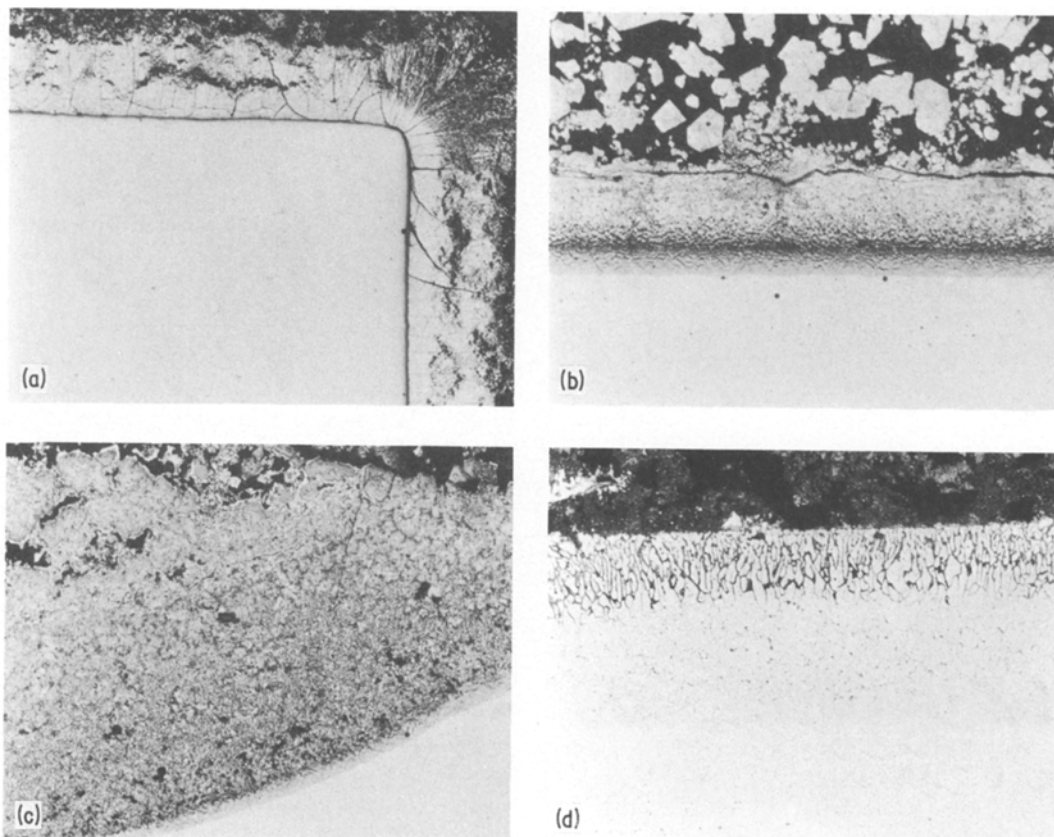


Figure 11 Nital etched cross-sections of molten zinc-steel samples produced and held in argon-hydrogen for 1 h,  $\times 57.6$ , (a) 500° C, (b) 700° C, (c) 750° C, (d) 850° C.

distortion and fissuring within the nickel depleted islands of the channel and island structure produced at 750 to 850° C could be due to a cushioning effect by liquid within the channels.

The depth of zinc penetration of AISI 304L revealed in this work by the various structural features summarized in Tables III and V, lie between values reported in the literature for

TABLE V Interaction data for steel heated in an argon-hydrogen mixture for 10 min before being contacted by zinc for 60 min

Interaction temperature (° C)	Average values (mm)			
	Erosion	Intermetallic layer	Interdiffusion zone	Total penetration
500	0.007	< 0.001	< 0.001	0.007
	0.011	< 0.001	< 0.001	0.011
700	0.071	0.167	0.073	0.311
	0.101	0.167	0.073	0.341
	Island and channel zone		Interdiffusion zone	Total penetration
750	0.573		0.021	0.594
	0.308		0.067	0.375
800	1.62			1.62
	1.61			1.61
850	0.146		0.302	0.488
	0.153		0.305	0.458

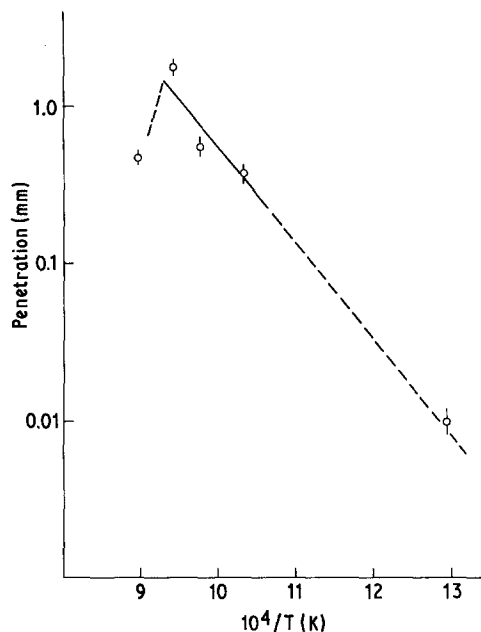


Figure 12 Plot of penetration data as a function of temperature for steel samples in contact with molten zinc for 1 h in argon-hydrogen.

AISI 316,\* 1 mm after 30 min at 750° C [12] and 0.03 mm after 700 h at 550° C [13], and AISI 321,\* 0.127 mm after 2 h at 816° C [11]. Nevertheless, the internal self consistency of the new penetration data leads us to believe that they provide a valid basis for assessing the effects of environment on the rates of molten zinc-steel interactions.

The most dramatic environmental effect observed during the programme was the inhibition of penetration by molten zinc due to carbon deposition when carbon monoxide atmospheres were used. The efficiency of the carbon as a barrier material was presumably a reflection of its chemical inertness toward and insolubility in zinc. While preventing zinc penetration, the use of carbon monoxide atmospheres caused some carburization of the steel and it is noteworthy, therefore, that Cottrell and Swan [8] observed carburizing atmospheres to inhibit or delay embrittlement by molten zinc at 800° C. These authors as well as Arrowsmith and Barnby [12] have also observed that oxide films on steel surfaces can prevent penetration by molten zinc during brief exposures, and this has been confirmed in the present pro-

TABLE VI Erosion of steel samples heated in contact with zinc oxide

Temperature (° C)	Time (min)	Erosion (mm)
700	30	0.041
	60	0.023
750	30	0.029
	60	0.005
780	30	0.098
	60	0.014
835	30	0.012
	60	0.018

gramme. However, calculations based on microbalance data suggest that quite substantial oxide films are needed to produce significant delays; the delays of 15 min at 850° C and 1.5 min at 700° C being associated with oxide films estimated to be 90 and 35 nm thick. The films formed on AISI 304L stainless steel in air at elevated temperatures are complex and it is a matter of speculation whether radically different and more protective oxides such as the alumina formed on Fecralloy®† steels would produce longer delays.

No inhibition effects were expected during the molten zinc interaction studies conducted in argon-hydrogen atmospheres and the cleanliness and complete wetting of the samples suggest that the expectation was realized. The reduced penetration in argon-hydrogen atmospheres observed at 850° C, therefore, is not thought to be inhibition by surface films but due to excessive take up of iron, chromium and especially nickel into the zinc which could reduce its activity and even produce partial solidification.

Interpretation of the zinc vapour and zinc oxide interaction data is more speculative because of its limited extent but some similarities with published data have been revealed. Thus, the etching characteristics of the pitted regions of our samples suggest that they were zinc rich and Cordwell [13] has recently observed the formation of  $Zn_3Ni$  on the surface of AISI 316 exposed to zinc vapour at 550° C. Similarly, Bennett *et al.* [16] observed pitting of AISI 304 steel samples exposed to zinc vapour at 900° C, but they attributed the effect to the leaching of nickel by condensed zinc droplets which ran off the vertical sample surfaces. While nickel leaching may have occurred, the pits produced

\*Typically, AISI 316 is Fe-18Cr-12Ni-2.8Mo-1.8Mn-0.5Si-0.05C-0.02S and AISI 321 is Fe-18.3Cr-10.1Ni-1.6Mn-0.45Ti-0.07C-0.02S.

†® Registered trade name.

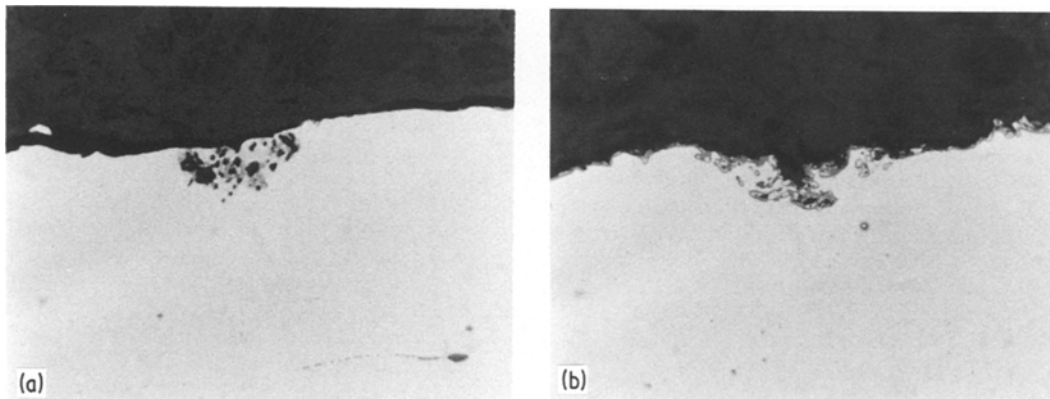
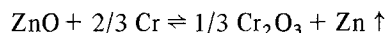


Figure 13 Surface and subsurface structures produced by exposing steel to zinc oxide for 60 min at (a) 700° C, and (b) 850° C. Etched in nital,  $\times 288$ .

on the horizontal surfaces of our samples cannot be attributed plausibly to the run off of droplets. The pitting produced by contact with zinc oxide in an argon–hydrogen atmosphere was similar to, but more extensive than, that observed on the zinc vapour interaction samples. This similarity may be significant in that zinc oxide could be reduced by chromium in the steel. The free energy of the reaction



is about  $-40 \text{ kJ}$  at the temperature of interest and substitution of the chromium activity of about 0.3 suggested by Campbell and Tyzack [17] for AISI 316 stainless steel leads to an estimate of the equilibrium zinc vapour pressure of more than sixty atmospheres. Since the boiling point of zinc is above the temperatures used in the interaction studies, zinc oxide is a source of both metal vapour and liquid and therefore, might produce intermetallic layers, interdiffusion zones and even channel and island structures in time. Such a reduction of zinc compounds to the metal might also be the cause of the zinc silicate embrittlement of a DIN 1.4541 steel (Fe–18 wt % Cr–10 wt % Ni–0.5 wt % Ti– $< 0.1 \text{ wt } \% \text{ C}$  reported by Herbsleb and Schwenk [18]). Thus while nickel has been found to play an important role in the interaction of stainless steel with molten zinc, the chromium activity of steels also could have a marked influence on their interaction with zinc oxide.

## 5. Conclusions

1. Molten zinc interacts with unstressed AISI 304L stainless steel in air to erode or penetrate from

0.003 to 1.7 mm in 1 h at 500 to 850° C. Penetration at 700 to 850° C produces mechanically detrimental structures such as cracked intermetallic layers, distorted and fissured interdiffusion zones and liquid channels.

2. Penetration at 850° C can be reduced by the prior growth of an oxide film on the steel surface, and deposits of carbon from carbon monoxide atmospheres can inhibit penetration of the steel by molten zinc for at least one hour at 850° C.

3. The extent of penetration by molten zinc suggests that no inhibiting oxide films are formed on the steel surfaces in argon–hydrogen atmospheres. The activation energy of the penetration process is about  $230 \text{ kJ mol}^{-1}$ .

4. Zinc vapour in air produces slight pitting of steel surfaces at 700 to 850° C, while zinc oxide in argon–hydrogen atmospheres produces extensive pitting and some erosion of the steel surfaces at 700 to 800° C, probably due to its reduction by chromium to form zinc vapour and liquid.

## Acknowledgements

Thanks are due to the Dutch State Mines who funded this study and to Drs Tuijnman and Leerschool for their interest and guidance. It is also a pleasure to acknowledge the contributions of Mr C. D. Kennedy who performed the electron probe microanalyser examinations and Dr C. F. Knights for a useful discussion on thermodynamics.

## References

1. J. E. CANTWELL and R. E. BRYANT, *Hydrocarbon Process*, May (1973) 114.
2. H. G. ORBONS, Appendix II of "The Flixborough Disaster" Report of the Court of Inquiry (HMSO, London, 1975).

3. "Technical Lessons of Flixborough" Meeting of the Nottingham Group of the Institution of Chemical Engineers, Nottingham University, Nottingham, December 1975, reported in *The Chemical Engineer*, February (1976) p. 119.
4. "Engineering Disasters" (London and Chilterns Metallurgical Societies, Hemel Hempstead, 1977).
5. "Zinc Embrittlement of Austenitic Stainless Steel", Health and Safety Executive Technical Data Note 53/1 (1976).
6. D. ELLIOTT, *Process Eng.* July (1976) 67.
7. S. SADIGH, *Mater. Performance* July (1981) 16.
8. A. H. COTTRELL and P. R. SWANN, *Chem. Eng.* April (1976) 266.
9. M. ANDREANI, P. AZOU and P. BASTIEN, *CR Acad. Sci. Paris* 263C (1966) 1041.
10. *Idem*, *Mem. Sci. Rev. Met.* 66 (1969) 21.
11. F. PAGE, *Amer. Electroplat. Soc.* 30 (1943) 436.
12. D. J. ARROWSMITH and J. F. BARNBY, in "The Flixborough Disaster" Report of the Court of Inquiry (HMSO, London, 1975).
13. J. E. CORDWELL, *Met. Sci.* 12 (1978) 352.
14. R. DE BACKER, A. PHOOGHE, P. MOYAERT, M. VICTORIA and A. VINCKIER, in "Proceedings of the Symposium on Corrosion and Mechanical Stress at High Temperatures" edited by V. Guttman and H. Herz (Applied Science Publishers, Barking, 1981) p. 405.
15. M. HANSEN, "Constitution of Binary Alloys" (McGraw-Hill, New York, 1958) p. 738 and p. 1060.
16. G. A. BENNETT, P. A. NELSON and L. BURRIS, *Trans. Met. Soc. AIME* 233 (1965) 1032.
17. C. S. CAMPBELL and C. TYZACK, Proceedings of the Symposium of Alkali Metal Coolants, Vienna, 1966 (IAEA, Vienna, 1966) p. 159.
18. G. HERBSLEB and W. SCHWENK, *Werkstoffe und Korrosion* 28 (1977) 145.

*Received 29 June  
and accepted 12 July 1982*